# Concurrent Multi-Mode Excitation for Mode Division Multiplexing over Substrate Integrated Waveguides

Mohamed H. A. Elsawaf<sup>#1</sup>, Constantine Sideris<sup>#2</sup>,

\*Ming Hsieh Department of Electrical and Computer Engineering, University of Southern California, USA

1 elsawaf@usc.edu, 2 csideris@usc.edu

Abstract — This article presents an approach for achieving a concurrent dual-channel link over a single substrate-integrated waveguide (SIW) by designing couplers to selectively excite the first two TE modes. The proposed design was fabricated and experimentally characterized to verify its performance. The  $TE_{10}$ and  $TE_{20}$  channels achieved a measured 4 GHz and 3 GHz 10-dB return loss fractional bandwidths (FBWs) from 11-15 GHz and from 10.2-13.2 GHz respectively. The insertion losses for  $TE_{10}$  and  $TE_{20}$  were less than 1.0 dB and 1.5 dB respectively with greater than 40 dB of isolation measured between the two channels. To the best of our knowledge, this is the first demonstration of a dual-mode SIW link for which both channels can be operated over the same frequency range. The 2.2 GHz of bandwidth overlap in addition to the high isolation between the two channels enables true full duplex communication for high-data rate chip-to-chip communication applications.

Keywords — full duplex, multimode, multichannel, substrate integrated waveguide (SIW).

### I. Introduction

Rapid advances in technology today have led to an ever increasing demand for faster and more efficient communication links. The majority of existing links are either optical or electrical depending on the distance [1]-[3]. Mid-range communication links (e.g., for server backend applications or chip-to-chip on-board interconnects) are an active area of research. In recent years, waveguides have attracted significant interest [4]-[6] due to their potential for high-data rate, low-loss communication over moderate distances without the need for expensive optical components, such as lasers, photodiodes, and modulators. In particular, substrate integrated waveguides (SIWs), which are the planar realization of conventional rectangular waveguides, inherit the low loss properties of conventional waveguides while simultaneously being easily fabricable using standard printed circuit board fabrication (PCB) techniques and offering improved integration with planar components [7]–[9].

An SIW can be realized using a conventional two-layer PCB, where the upper and lower metals of the laminate act as the top and bottom walls respectively. The side walls are realized by inserting multiple metal posts (vias) with small sub-wavelength separation. Such waveguides have been used to realize a plethora of components including filters/duplexers [10], power dividers/combiners [11], and antennas [12], [13]. Additionally, their viable design frequency range extends all the way up to the sub-THz regime [4], [6], making SIWs a good candidate for fast and efficient mid-range communication links.

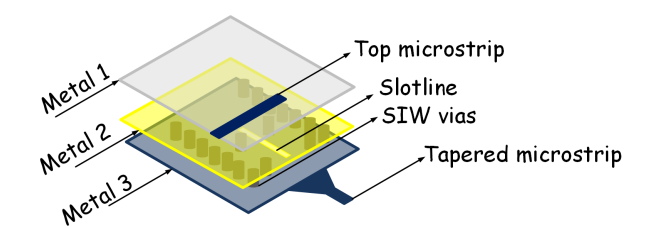


Fig. 1. Layer schematic diagram of the proposed excitation structure.

The fundamental mode  $(TE_{10})$  excitation of SIWs has been thoroughly investigated using various planar transmission lines such as: microstrip [9], coplanar waveguide (CPW) [14], stripline [15], and grounded CPW (GCPW) [16]. Recently, various higher-order mode excitation techniques have been proposed as well to enhance overall channel bandwidth including exciting the  $TE_{20}$  mode by using a slotline [17]. However, the only previously reported multi-mode implementation [18] did not support excitation of both modes over the same frequency range, requiring each mode to be used in a different band. In this article, we present a design which supports concurrent dual-mode excitation of the  $TE_{10}$  and  $TE_{20}$  modes of an SIW over the same frequency range while maintaining very high isolation between the two channels. This greatly simplifies the transceiver design required and can be used to achieve true full-duplex communication, enabling new horizons for building practical systems which leverage both mode-division multiplexing as well as frequency division multiplexing (FDM). To the best of our knowledge, this is the first demonstration of a dual-mode SIW where both modes can be operated concurrently over the same frequency band. The proposed structure has been designed and fabricated using 4-layer PCB technology on Rogers (RT Duroid 5880) laminates with  $(h = 0.508 \text{ mm}, \epsilon_r = 2.2, tan\delta = 0.004)$ .

## II. MODE EXCITATION

Fig. 1 shows a schematic diagram of the full proposed structure and its constituent layers. The design is built by stacking two laminates on top of each other. The bottom metal of the top laminate is fully-etched out. The SIW itself is realized in the bottom substrate between metals 2 and 3. The fundamental mode of the SIW is excited by using a tapered microstrip to SIW transition etched in metal 3. The second order mode  $(TE_{20})$  is excited by using a slotline to SIW transition similar to the approach used in [17]. The slotline

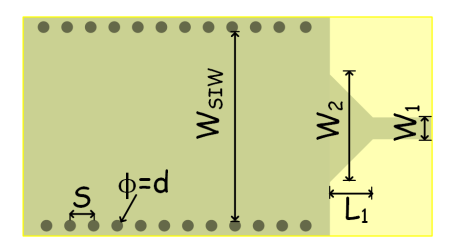


Fig. 2. Schematic of the fundamental mode excitation structure.

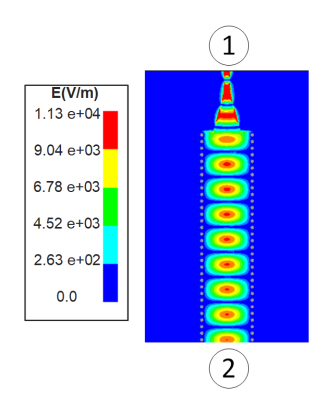


Fig. 3. Electric field profile of the microstrip to SIW transition showing  $TE_{10}$  mode launching. Port 1 is the microstrip port, and port 2 is a waveport terminating the SIW.

itself is etched in metal 2 (the top metal of the SIW) and is fed via a microstip to slotline transition (etched on the top metal 1).

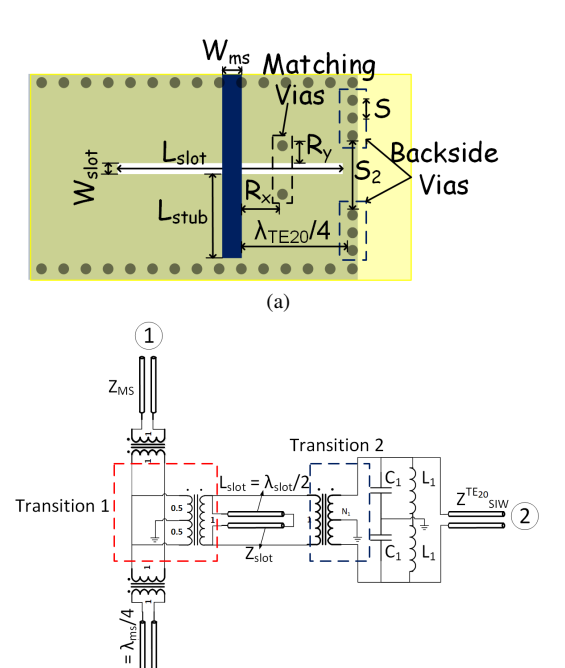
## A. Fundamental ( $TE_{10}$ ) Mode Excitation

The fundamental mode of the SIW structure is the conventional  $TE_{10}$  mode. To excite this mode, a field (energy) source should be placed at the center of the guide, and a suitable matching technique should be used to match this source to the guide. Several structures have been investigated to excite and match this mode in the literature [14]–[16]. In this work, the source of excitation is a conventional microstrip line, which launches power to the mode maximum at the center of the SIW. This microstrip is matched to the SIW by adiabatically tapering it (gradual change of impedance) to match its impedance  $Z_0$  to the SIW's  $TE_{10}$  modal impedance,  $Z_{SIW}$  [19]. A 2D schematic of the exciting structure is shown in Fig. 2.

The design of the exciting structure starts by choosing the width of the SIW which is given by

$$W_{SIW} = W - (\frac{d^2}{0.95S}),\tag{1}$$

where W is the width corresponding to half-wavelength at the desired cutoff frequency (5 GHz), i.e.  $\lambda = \frac{c}{f \times \sqrt{\epsilon_r}}$ , and  $\epsilon_r = 2.2$ . The parameters d and S are the diameter and spacing of the SIW vias respectively, which are both are chosen as 1 mm in this design. The width  $W_1$  is chosen to achieve a 50  $\Omega$  microstrip impedance, and  $L_1$  and  $W_2$  are tuned simultaneously to maximize the matching level and bandwidth.



(b) Fig. 4.  $TE_{20}$  exciting structure (a) Schematic, (b) Equivalent circuit model.

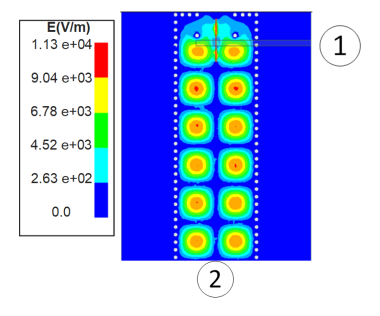


Fig. 5. Electric field profile of the  $TE_{20}$  mode launched using a slotline fed by a microstrip line.

They provide a smooth transition from the 50  $\Omega$  impedance to the  $Z_{SIW}$  of the waveguide given by:

$$Z_{SIW} = \frac{K\eta}{\beta} \tag{2}$$

$$K^2 = \beta^2 + K_c^2 \tag{3}$$

where K is the plane-wave propagation constant in the dielectric,  $\beta$  is the guided propagation constant, and  $\eta$  is the propagation impedance in the dielectric. The relation between K and  $\beta$  is given in (3). The excitation structure is simulated in ANSYS HFSS with the exciting microstrip (port 1) on one side of the SIW and a terminating waveport on the other side as illustrated in Fig. 3, which shows the modal profile excited by the structure.

# B. Higher Order Mode ( $TE_{20}$ ) Excitation

The first higher order mode of the SIW is  $TE_{20}$ . It can be thought of as two fundamental modes concatenated

Table 1. Dimensions of the Proposed Structure

Parameter	Length (mm)		
d	1 mm		
$L_1$	9 mm		
$L_{slot}$	13 mm		
$L_{stub}$	5.4 mm		
$R_x$	5.5 mm		
$\frac{R_y}{S}$	6 mm		
S	1 mm		
$W_1$	1.6 mm		
$W_2$	6 mm		
$W_{SIW}$	22 mm		
$W_{ms}$	1.6 mm		
$W_{slot}$	0.3 mm		
$S_2$	10 mm		

anti-symmetrically ( $\pi$  phase shift). The excitation strategy for this mode follows the work in [17], where a slotline, which has a similar anti-symmetric field profile, is used to launch the mode. The slotline itself is fed via a microstrip to slotline transition. The schematic and the equivalent circuit model of the proposed excitation structure are illustrated in Fig. 4. The circuit model, shown in Fig. 4b, shows a microstrip/slotline transition encircled in red. The microstrip section before the slotline  $(Z_{MS})$  is matched to 50  $\Omega$ , and a transformer is used to model the microstrip-slotline junction [20]. A microstrip stub extends for a quarter-wavelength ( $L_{stub} = \lambda_1/4$ ) beyond the junction and is open ended. On the other end of the transformer, the slotline, which is etched on the top metal of the SIW and is shorted on both ends acts as a half-wavelength resonator to efficiently couple into the waveguide. Its width (0.3 mm) is chosen to be the minimum allowed by the fabrication constraints to minimize radiation losses (insertion loss). This width corresponds to  $Z_{slot} = 160 \ \Omega$ .

The second transition (circled in blue in Fig. 4b) from the slotline to the SIW is also modeled by a transformer [17]. The SIW's capacitive modal input impedance,  $Z_{SIW}^{TE_{20}}$ , is modeled by the two  $C_1$  capacitors. Two vias (circled in black in Fig. 4a) are inserted in the SIW, which act as inductors (modeled by  $L_1$  in the circuit) and improve the matching of this transition. Furthermore, two lines of vias on the backside (encircled in blue in Fig. 4a) are placed a quarter-wavelength away from the microstrip/slotline junction, to act as directors/back reflectors for the electric field. They also further improve the matching [17]; however, the gap between them (labeled " $S_2$ ") must be larger than  $W_2$  in Fig. 2 in order to not adversely affect the  $TE_{10}$  excitation. The excitation structure is verified using ANSYS HFSS with port 1 as the microstrip port, and port 2 as a terminating waveport as shown in Fig. 5, which also shows the excited modal profile. The dimensions of the exciting structure are reported in Table 1.

## III. EXPERIMENTAL RESULTS

The fabricated structure is shown in Fig. 6. The structure is fabricated by stacking two Rogers Duroid 5880 ( $h=0.508~\mathrm{mm},~\epsilon_r=2.2r,~tan\delta=0.004$ ) laminates on top of each other using a Rogers 4450 ( $h=0.1~\mathrm{mm},~\epsilon_r=3.2,~tan\delta=0.004$ )

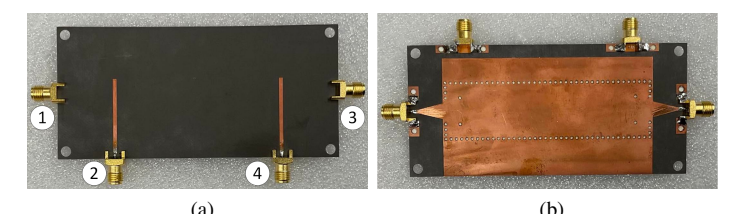


Fig. 6. Fabricated structure (a) Top side, (b) Bottom side.

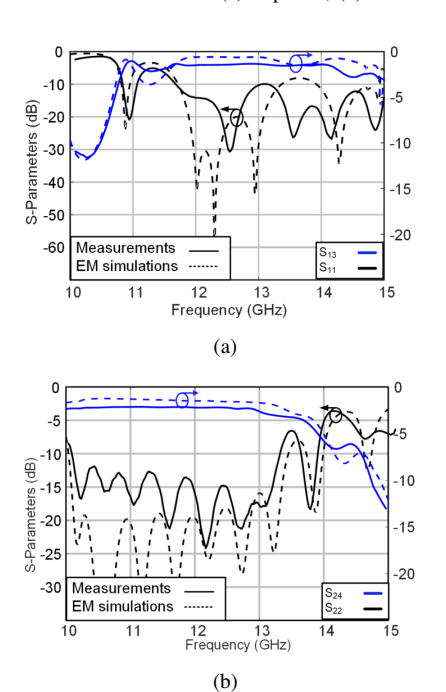


Fig. 7. Measured S-parameters (a) Return loss and insertion loss from port 1, and (b) return and insertion loss from port 2.

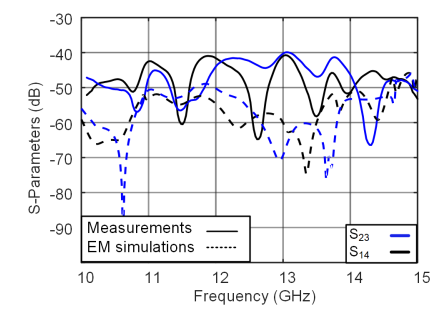


Fig. 8. Cross-modal isolation.

0.006) prepreg. The length of the fabricated SIW is  $4\lambda$  ( $\approx 80$  mm), where  $\lambda$  is the cut-off wavelength of  $TE_{20}$  mode (10 GHz), and the width of the whole structure is  $1\lambda$ . The ports are defined according to Fig. 6a, where ports 1 and 3 excite the  $TE_{10}$  mode and ports 2 and 4 excite the  $TE_{20}$  mode.

The measured and simulated insertion and return loss of the structure when excited by port 1 ( $TE_{10}$ ) are shown in Fig. 7a, indicating that the return loss (RL) ( $S_{11}$ ) remains at or below 10-dB between 11.8-15 GHZ, corresponding to a 3.2 GHz FBW. The structure has roughly 1 dB insertion loss (IL) ( $S_{13}$ ) with almost the same 3-dB BW as the 10-dB return-loss

Table 2. Comparison against prior work

	[18]	[17]	[16]	This Work
Modes excited	$TE_{10}$ and $TE_{20}$	$TE_{20}$	$TE_{10}$	$TE_{10}$ and $TE_{20}$
Frequency-range (GHz)	(10-20)	(7.5-13)	(26-32)	(10-15)
Exciting Structure	Microstrip line	slotline	GCPW	Microstrip and slot lines
10-dB return-loss FBW <sup>1</sup>	22%	45.5%	25%	30%
Insertion-loss (dB)	1	2.6	0.5	1.5
Multi-mode coupling (max/min dB)	(45/5)	N/A	N/A	(62/40)
Multi-mode Multiplexing possibility	No	No	No	Yes

<sup>&</sup>lt;sup>1</sup> FBW is calculated with respect to the highest cut-off frequency available.

FBW. The measurement results for exciting port 2 ( $TE_{20}$ ) are shown in Fig. 7b, showing a measured 10-dB return-loss FBW of 3 GHz (10.1-13.1 GHz) and 1.5 dB insertion-loss ( $S_{24}$ ) with a 3 GHz (10-13 GHz) 3-dB BW. The excess 0.5 dB of insertion loss may be due to the lossy nature of the exciting slotline.

The measured and simulated cross-modal isolation  $(S_{14})$  and  $(S_{23})$  are plotted in Fig. 8. They isolation remains greater than 40 dB for both modes between 10-15 GHz. Comparing this cross-modal isolation to the isolation between two adjacent single-mode SIW's sharing a common wall, the isolation achieved is more than 10 dB larger, which is crucial for reducing inter-channel interference.

Table 2 compares this work with previous state-of-the-art works. Note that the present work is the only realization which realizes excitation of two modes concurrently over the same frequency range. Despite the additional complexity of concurrent multi-mode excitation, the performance achieved compares quite favorably to prior art, having the largest 10 dB FBW and isolation and comparable IL.

### IV. CONCLUSION

This paper presented for the first time concurrent multi-mode excitation of SIW over the same frequency band. This opens the horizon for increasing available communication bandwidth via mode-division multiplexing to increase the channel capacity without requiring increased complexity in transceiver design. The proposed structure efficiently excites the first two modes of the SIW in a 3 GHz (10-13 GHz) band, with a low IL and high cross-modal isolation. The structure has been fabricated and the measurement results show close agreement with EM simulations.

## ACKNOWLEDGMENT

The authors are grateful for support by the National Science Foundation (CCF-2047433, ECCS-2133138). The authors would like to thank Dr. Alessandro Maggi and Mr. Vinay Chenna for their assistance with the measurements.

## REFERENCES

- C. A. Thraskias et al., "Survey of Photonic and Plasmonic Interconnect Technologies for Intra-Datacenter and High-Performance Computing Communications," *IEEE Commun. Surveys Tut.*, vol. 20, no. 4, pp. 2758-2783.
- [2] J. W. Holloway, G. C. Dogiamis and R. Han, "Innovations in Terahertz Interconnects: High-Speed Data Transport Over Fully Electrical Terahertz Waveguide Links," *IEEE Microw Mag.*, vol. 21, no. 1, pp. 35-50, Jan. 2020.
- [3] Q. J. Gu, "THz interconnect: The last centimeter communication," *IEEE Commun. Mag.*, vol. 53, no. 4, pp. 206–215, 2015.
- [4] K. Dhwaj, Y. Zhao, R. A. Hadi, X. Li, F. M.-C. Chang, and T. Itoh, "A 0.55 THz on-chip substrate integrated waveguide antenna," in *Proc. 43rd Int. Conf. Infr., Millim., Terahertz Waves (IRMMW-THz)*, Sep. 2018, pp. 6–7.
- [5] J. W. Holloway, G. C. Dogiamis, S. Shin and R. Han, "220-to-330-GHz Manifold Triplexer With Wide Stopband Utilizing Ridged Substrate Integrated Waveguides," *IEEE Trans. Microw. Theory Techn.*, vol. 68, no. 8, pp. 3428-3438, Aug. 2020.
- [6] Y. Shang, H. Yu, H. Fu, and W. M. Lim, "A 239–281 GHz CMOS receiver with on-chip circular-polarized substrate integrated waveguide antenna for sub-terahertz imaging," *IEEE Trans. THz Sci. Technol.*, vol. 4, no. 6, pp. 686–695, Nov. 2014.
- [7] H. Uchimura, T. Takenoshita, and M. Fujii, "Development of a 'laminated waveguide'," *IEEE Trans. Microw. Theory Techn.*, vol. 46, no. 12, pp. 2438–2443, Dec. 1998.
- [8] D. Deslandes and K. Wu, "Accurate modeling, wave mechanisms, and design considerations of a substrate integrated waveguide," *IEEE Trans. Microw. Theory Techn.*, vol. 54, no. 6, pp. 2516–2526, Jun. 2006.
- [9] D. Deslandes and K. Wu, "Integrated microstrip and rectangular waveguide in planar form," *IEEE Microw. Wireless Compon. Lett.*, vol. 11, no. 2, pp. 68–70, Feb. 2001.
- [10] J.-H. Lee, N. Kidera, G. DeJean, S. Pinel, J. Laskar, and M. M. Tentzeris, "A V-band front-end with 3-D integrated cavity filters/duplexers and antenna in LTCC technologies," *IEEE Trans. Microw. Theory Techn.*, vol. 54, no. 7, pp. 2925–2936, Jul. 2006.
- [11] K. Sakakibara, Y. Kimura, A. Akiyama, J. Hirokawa, M. Ando, and N. Goto, "Alternating phase-fed waveguide slot arrays with a single-layer multiple-way power divider," in *IEEE Proc.-Microw., Antennas Propag.*, vol. 144, no. 6, pp. 425–430, Dec. 1997.
- [12] Y. J. Cheng, W. Hong, and K. Wu, "Design of a monopulse antenna using a dual V-type linearly tapered slot antenna (DVLTSA)," *IEEE Trans. Antennas Propag.*, vol. 56, no. 9, pp. 2903–2909, Sep. 2008.
- [13] F. Xu, K. Wu, and X. Zhang, "Periodic leaky-wave antenna for millimeter wave applications based on substrate integrated waveguide," *IEEE Trans. Antennas Propag.*, vol. 58, no. 2, pp. 340–347, Feb. 2010.
- [14] F. Taringou, D. Dousset, J. Bornemann, and K. Wu, "Broadband CPW feed for millimeter-wave SIW-based antipodal linearly tapered slot antennas," *IEEE Trans. Antennas Propag.*, vol. 61, no. 4, pp. 1756–1762, Apr. 2013.
- [15] K. Kim, J. Byun, and H. Y. Lee, "Substrate integratewaveguide quasi Yagi antenna using SIW-to-CPS transition for low mutual coupling," in Proc. IEEE AP-S Int. Symp. Dig., Jul. 2010, pp. 1–4.
- [16] D. Deslandes and K. Wu, "Analysis and design of current probe transition from grounded coplanar to substrate integrated rectangular waveguides," *IEEE Trans. Microw. Theory Techn.*, vol. 53, no. 8, pp. 2487–2494, Aug. 2005.
- [17] P. Wu, J. Liu and Q. Xue, "Wideband Excitation Technology of TE20 Mode Substrate Integrated Waveguide (SIW) and Its Applications," *IEEE Trans. Microw. Theory Techn.*, vol. 63, no. 6, pp. 1863-1874, June 2015.
- [18] A. Suntives and R. Abhari, "Design and application of multimode substrate integrated waveguides in parallel multichannel signaling systems," *IEEE Trans. Microw. Theory Techn.*, vol. 57, no. 6, pp. 1563–1571, Jun. 2009.
- [19] D. M. Pozar, Microwave Engineering, 3rd ed. New York, NY, USA: Wiley, 2005.
- [20] A. M. H. Nasr, A. M. E. Safwat and H. Elhennawy, "Via-free microstrip to slotline baluns using slotted microstrip cross-junction," in Proc. Eur. Microw. Conf. (EuMC), 2017, pp. 85-88.